

# REGULATORY INFORMATION DISTRIBUTION SYSTEM (RIDS)

ACCESSION NBR: 8201070059 DOC. DATE: 81/12/22 NOTARIZED: NO DOCKET #  
 FACIL: 50-397 WPPSS Nuclear Project, Unit 2, Washington Public Power 05000397  
 AUTH. NAME: AUTHOR AFFILIATION  
 BOUCHY, G.D. Washington Public Power Supply System  
 RECIP. NAME: RECIPIENT AFFILIATION  
 SCHWENCER, A. Licensing Branch 2

SUBJECT: Forwards responses to open items discussed at 811117-18  
 Geosciences meeting. Remaining responses will be transmitted  
 prior to 811231.

DISTRIBUTION CODE: B001S COPIES RECEIVED: LTR 1 ENCL 60 SIZE: 32  
 TITLE: PSAR/FSAR AMDTS and Related Correspondence

NOTES: 2 copies all matl: PM.

05000397

ACTION:	RECIPIENT ID CODE/NAME	COPIES		RECIPIENT ID CODE/NAME	COPIES	
		LTTR	ENCL		LTTR	ENCL
ACTION:	A/D LICENSNG	1	0	LIC BR #2 BC	1	0
	LIC BR #2 LA	1	0	AULUCK, R. 01	1	1
INTERNAL:	ELD	1	0	IE	06	3
	IE/DEP/EPDB 35	1	1	IE/DEP/EPLB 36	3	3
	MPA	1	0	NRR/DE/CEB 11	1	1
	NRR/DE/EOB 13	3	3	NRR/DE/GB 28	2	2
	NRR/DE/HGEB 30	2	2	NRR/DE/MEB 18	1	1
	NRR/DE/MTEB 17	1	1	NRR/DE/QAB 21	1	1
	NRR/DE/SAB 24	1	1	NRR/DE/SEB 25	1	1
	NRR/DHFS/HFEB40	1	1	NRR/DHFS/LQB 32	1	1
	NRR/DHFS/OLB 34	1	1	NRR/DHFS/PTRB20	1	1
	NRR/DSI/AEB 26	1	1	NRR/DSI/ASB 27	1	1
	NRR/DSI/CPB 10	1	1	NRR/DSI/CSB 09	1	1
	NRR/DSI/ETSB 12	1	1	NRR/DSI/ICSB 16	1	1
	NRR/DSI/PSB 19	1	1	NRR/DSI/RAB 22	1	1
	NRR/DSI/RSB 23	1	1	NRR/DST/LGB 33	1	1
		REG FILE 04	1	1		
EXTERNAL:	ACRS 41	16	16	BNL (AMDTS ONLY)	1	1
	FEMA-REP DIV 39	1	1	LPDR 03	1	1
	NRC PDR 02	1	1	NSIC 05	1	1
	NTIS	1	1			

TOTAL NUMBER OF COPIES REQUIRED: LTTR

65 60  
 63 ENCL 58

28



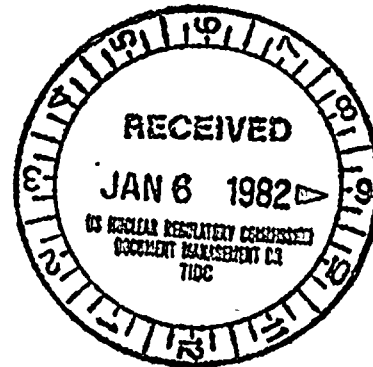
## Washington Public Power Supply System

P.O. Box 968 3000 George Washington Way Richland, Washington 99352 (509) 372-5000

December 22, 1981  
G02-81-541  
SS-1-02-CDT-81-111

Docket No. 50-397

Mr. A. Schwencer, Director  
Licensing Branch No. 2  
Division of Licensing  
U.S. Nuclear Regulatory Commission  
Washington, D.C. 20555



Dear Mr. Schwencer:

Subject: NUCLEAR PROJECT NO. 2  
GEOSCIENCES BRANCH OPEN ITEMS

Reference: Letter, A. Schwencer to R.L. Ferguson,  
"WNP-2 Request for Additional Information",  
dated December 1, 1981

Enclosed are sixty (60) copies of the completed responses to the open items discussed at the Geosciences meeting on November 17-18, 1981. The remaining responses will be transmitted to the NRC prior to December 31, 1981.

Very truly yours,

*G. D. Bouchev for*

G. D. Bouchev  
Deputy Director, Safety & Security

CDT/jca  
Enclosures

cc: R Auluck - NRC  
I Alterman - NRC  
J Kimball - NRC  
WS Chin - BPA  
R Feil - NRC Site

1300/  
51/60

8201070059 811222  
PDR ADDCK 05000397  
A PDR



Q. 360.015

Concerning the Wallula Gap fault near Yellepit:

- a. Provide an explanation of the difference in age of the Kennewick fanglomerate as reported in FSAR amendment 18, Section 2.5.1.2.4.5 on p. 2.5-96 and in Appendix 2.5N.8.1.6.
- b. Was the block of ash that was observed in the down dropped block at the fault in the Yellepit trench dated? If so, what age has been determined for it? If not, are there samples of that ash presently available for dating?

Response:

- a. Based on the most recent calculations by Dr. T.L. Ku, the more correct age of the Kennewick fanglomerate is "at least 20,000 years old." Early in 1981, Woodward-Clyde Consultants learned that the age of the Kennewick fanglomerate given in Woodward-Clyde Consultants report "WPPSS 1872 Earthquake studies", July 1978, was regarded by Dr. Ku, who made the original age calculation, as being incorrect.

On February 26, 1981, J.H. Black spoke to Professor Ku about a possible discrepancy in the age of the caliche that had been dated using the uranium-thorium method. Professor Ku reported that an error had been made in calculating the age of sample B, and that the sample should be regarded as at least  $21 \pm 4 \times 10^3$  years old as cited in the above report. A copy of the telephone conversation record which documents this discussion with Dr. Ku is appended.

- b. The only known occurrence of volcanic ash in the Yellepit trench was reported by S.M. Farooqui in the WNP-1/4 PSAR Amendment 23, October 1977, pp 2RH.4-2 to -4. Section 4.2.3.1 contains a description of the ash unit as follows:

"A lens of white ash, about 15 feet long and 2 to 6 inches thick, occurs in the loess just above the top of the gravel bed near Sta 0+12. Trace elements and petrographic analysis of a sample (PA1-48) of this ash indicates a Mt. Mazama affinity (see Subappendix 2RH-b)."

Subappendix 2RH-b presents geochemical and petrographic analyses of the volcanic ash:

1. Report on Volcanic Ash Samples, by M.H. Beeson.  
Five samples of ash, including PA1-48, from the Yellepit trench were analyzed.  
Hydration rinds were absent from four of the samples, but present in sample PA1-48, suggesting that this is younger than the other four.  
All the other four samples were taken from the Touchet beds. (Sample PA1-48 presumably is younger than the Touchet beds.)
2. Report of Petrographic Analyses of Ash Samples, by R.O. Van Atta indicates that five samples from the study area (Pasco Basin, including Yellepit trench), plus one from Mt. Mazama were analyzed. All were similar in concentrations of Lanthanum and Samarium (see Fig. 2RH-b-1) and were distinct from St. Helens' "S" and St. Helens' "J". It was concluded that all could be from a Mt. Mazama source.

The ash overlies the Kennewick fanglomerate, which is unfaulted. The age of the Kennewick fanglomerate has been estimated (see response to part "a" of this question) to be at least 20,000 years old. Van Atta (see above) concludes that the ash is probably younger than ashes taken from the Touchet beds dated at approximately 13,000 years P.B. (Mullineaux and others, 1977). Beeson (above) concludes that the ash could be from a Mt. Mazama source, dated at approximately 7,000 years B.P. (Davis, 1978).

In addition to the volcanic ash encountered at Station 0+12, there is a block of light colored tuff located near Station 2+70. The tuff occurs within the basal part of the fanglomerate and overlies the eroded surface of Umatilla basalt, a Tertiary basalt. A similar tuff that crops out as an interbed within the basalt sequence is exposed in the north face of the trench near Station 3+20. Based on the lithologic similarity between the tuff fragment in the fanglomerate and the tuff interbed and on their close proximity, the block found at Station 2+70 is concluded to have been derived from the interbed which is regarded by Farooqui, 1977 (Fig. 2RH.4-8), as belonging to the Selah Member. The Selah interbed underlies the Pamona Formation, which is about 12 million years old.

These relationships are still exposed and were examined by the NRC staff during a site review on December 9, 1981. Based on this field review, it was concluded that it is not necessary to sample and analyze the tuff exposed in the Yellepit trench.

References:

Farooqui, S.M., 1977, Geologic Studies of the Wallula Gap Fault as exposed in the trench: Subappendix 2RH to WNP-1/4 PSAR Amendment 23.

Davis, J.O., 1978, Quaternary tephronchronology of the Lake Lahontan area, Nevada and California: Nevada Survey, Archeological Research Paper No. 7.

Mullineaux, D.R., Wilcox, R.E., Ebaugh, W.F., Fryxell, R., and Rubbing, M., 1977, Age of the last major scabland flood of Eastern Washington, as inferred from associated ash beds of Mount St. Helens Set S: Geological Society of America Abstracts with Programs, p. 1105.





TELEPHONE CONVERSATION

14940-~~4140~~  
4143.2

14940-4140

Date: 26 Feb 81 Task No.: 1430

Location: SFO → LA

Participants: J. Black

Prof. Richard Ku (213) 743 - 6051

Subject: ① Performance of age dating caliche deposits from Pasco (3)  
② Revision of dates from WCC 1978 study

Significant Information or Decisions:

① (a) Norma Biggar's 5 samples. First by mid-April

(b) Then ours

Only other lab is USGS Denver - not available

Counter being repaired.

Cannot promise. Del. not March. Poss. April

Cost: \$ 450/ sample.

② Age date of sample B (See Report 13891 A/ July 1978;  
Appendix B — WPPSS 1872 E/Q studies) was incorrectly  
calculated: should be  $21 \pm 4 \times 10^3$  yrs NOT  $55 \pm 5 \times 10^3$  yrs

Action Items (with Target Dates):

① • Send samples anyway: Ku will advise in 2/3 weeks  
if can do the tests. Send to: Prof. R Ku at home

3613 Purdue Ave LA, CA 90066 (home).

② Advise Tom Turcotte of revised dates

Recorded by: J Black

11:45 / 26 Feb 81

Q. 360.016

In a report prepared for the U.S. Corps of Engineers (Stemmons and O'Malley, 1979-1980):

- a. Figures 20a and 20b are from Vansycle Canyon: Have the youthful-appearing faceted spurs having linear character been investigated for possible young age and, therefore, capability? What is the explanation for this feature?
- b. Figures 21a and 21b taken South of Umapine: Has the pronounced escarpment on the lower third of the hill in the center/upper right of 21a and in the center/right of 21b been investigated for possible recent movement? What is the explanation for this feature?

Response:

The origin of the faceted spurs east of Wallula Gap was investigated as part of the trenching and mapping investigation of the Wallula Gap fault (Woodward-Clyde Consultants, 1981). A regional reconnaissance was made of the lineaments and faceted spurs between Wallula Gap and Warm Springs Canyon, including the Vansycle Canyon lineament and three trenches were excavated across the Wallula fault southeast of Warm Springs Canyon (Figure 360.016-1). Based on these studies, the faceted spurs are interpreted to be the result of differential erosion across geologic contacts (both depositional and fault contacts) between different basalt flow units. The scarps south of Umapine were not specifically investigated as part of this study.

Lineament no. 1 near Warm Springs Canyon (Figure 360.016-2) is defined by an alignment of north facing faceted spurs and a broad bench that lies immediately north of the break in slope at the base of the spurs. Lineament no. 1 is coincident with the Wallula Gap fault. The bases of the higher and more-pronounced faceted spurs along lineament no. 2 are approximately coincident with the contact between the upper and lower units of the Frenchman Springs Member.

The Frenchman Springs lower unit, which occurs to the north of lineament no. 2 consists of an interbedded sequence of two distinctly different textural basalt types. The first type consists of dark black basalt that has very fine microphenocrysts in an aphanitic ground mass. This basalt breaks into equant clasts less than 15 cm in diameter. The first basalt type is interbedded with a second type that has a fine-grained ground mass and no aphanitic ground mass. The second basalt type commonly fractures into coarse joint blocks that are typically greater than 0.3 m in diameter. Coarse (>0.6 m) columnar joints



having well-developed partings perpendicular to the long axes of the columns are common. These two textural types are typically separated by thin gray vesiculated zones; locally the two basalt types grade laterally into one another.

The upper unit of the Frenchman Springs Member, which occurs on the south side of lineament no. 2 and underlies the spurs, consists of massive basalt flows that are petrographically similar to the fine-grained (non-aphanitic) rocks in the lower unit.

Figure 360.6-3 is a schematic cross section showing the relationship between the lineaments (faceted spurs) and the bedrock geology. Lineament no. 2, which is geomorphically similar to the lineament along Vansycle Canyon, is clearly not the result of recent tectonic displacement. In places, the break in slope at the base of the faceted spurs lies more than 400 m west of the Wallula Gap fault. The faceted spurs are the result of differential erosion across the depositional contact between the upper and lower units of the Frenchman Springs Member. The subparallel alignment and relative position of lineament no. 2 to the Wallula Gap fault may be indirectly related to displacement on the fault. If so, the faceted spurs are erosional fault-line features and the distance between the fault trace and the base of the spurs attests to the long time that would have been required to backwaste the scarp. Trenches across the Wallula Gap fault near Warm Springs showed that there has been no displacement since deposition of the late Pleistocene Touchet deposits (13,000 years B.P.). Trenches across the Wallula Gap fault at Yellepit indicate there has been no displacement during at least the past 20,000 years.

Detailed geologic mapping of the Vansycle Canyon area shows that the lineament along Vansycle Canyon (Slemmons and O'Malley, 1980, Figure 20b) may be either a fault scarp or a fault line erosional scarp. The faceted spurs between Vansycle Canyon and Wallula Gap are coincident with a breccia zone that defines the Wallula Gap fault. Both sets of faceted spurs are underlain by the Frenchman Springs Member. Although the faceted spurs shown in the report by Slemmons and O'Malley (1980) [i.e., Figures 20a, 20b, 21a and 21b] have not been trenched, the detailed mapping and trenching near Warm Springs Canyon and the trench at Yellepit indicates that faceted spurs are not a priori evidence for recent tectonic displacement. They are most likely the result of differential erosion across contacts (either depositional or fault contacts) between different flow units.



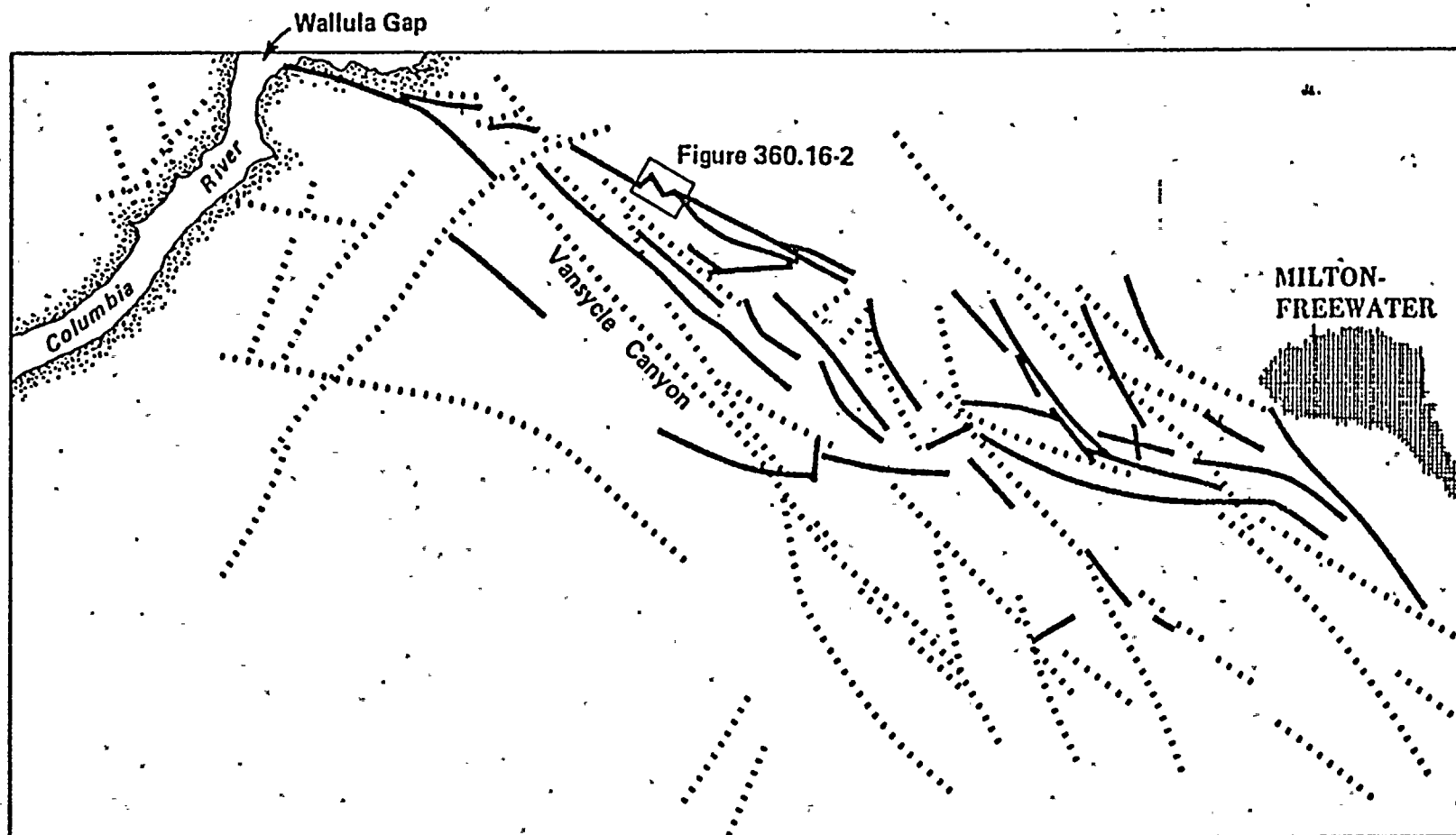
References:

Slemmons, D.B. and O'Malley, 1980, Fault and Earthquake hazard Evaluation of Five U.S. Corps of Engineers Dams in Southeastern Washington: Report prepared for U.S. Corps of Engineers, Seattle district, 60 pp.

Woodward-Clyde Consultants, 1981, Wallula Fault Trenching and Mapping: Draft report prepared for Washington Public Power Supply System, Richland, WA.



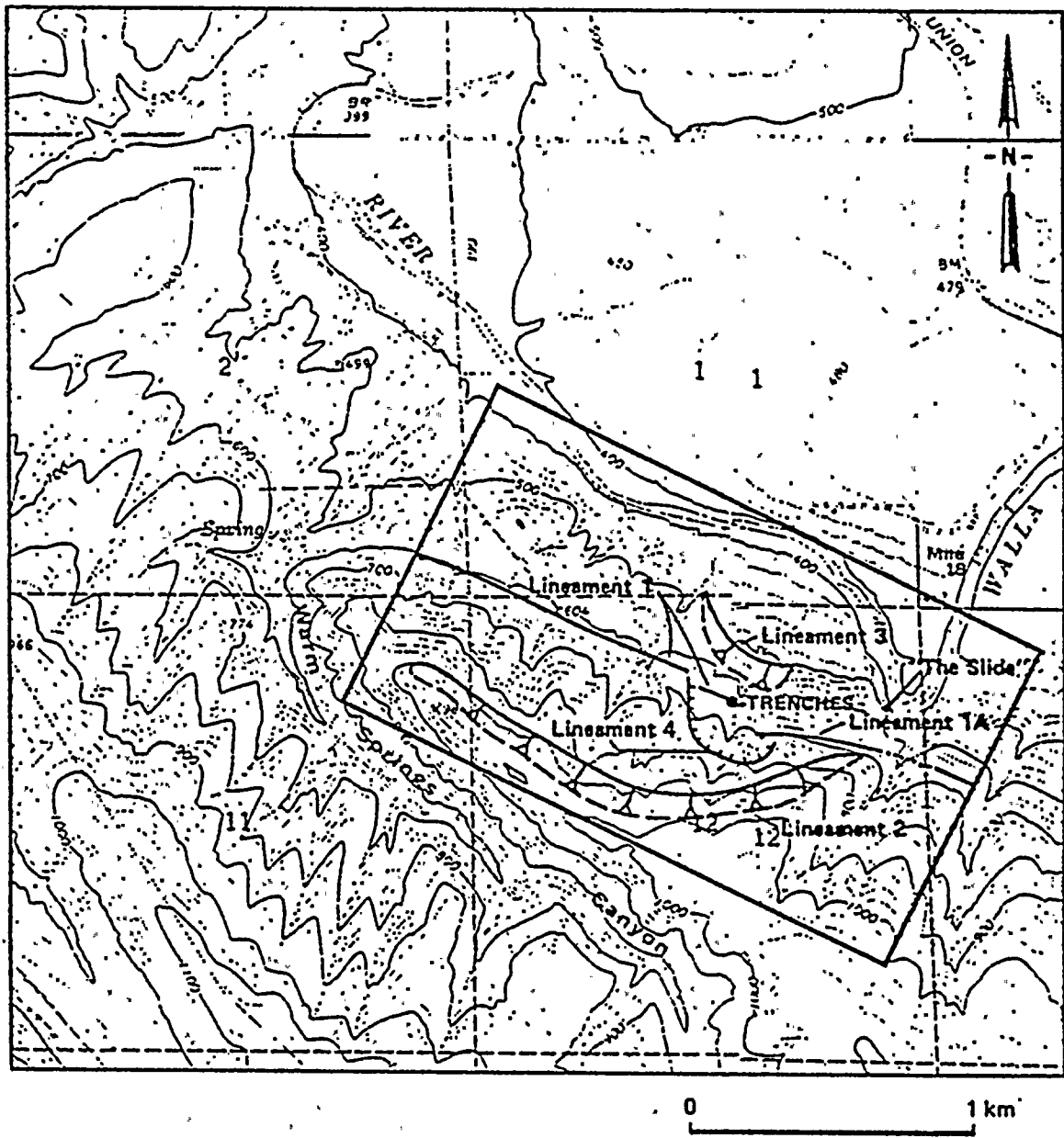
<p>WASHINGTON PUBLIC POWER SUPPLY SYSTEM Nuclear Project No. 2</p>	<p>PHOTOGEOLOGICAL INTERPRETATION OF LINEAMENTS AND POSSIBLE CAPABLE FAULTS BETWEEN WARM SPRINGS CANYON AND MILTON-FREEWATER</p>	<p>Figure 360.16-1</p>
--	--	----------------------------



Photogeological interpretation of lineaments (dashed) and possible capable faults (solid) between Warm Springs Canyon and Milton-Freewater. (From Slemmons and O'Malley, 1981, figures 15 and 17.)

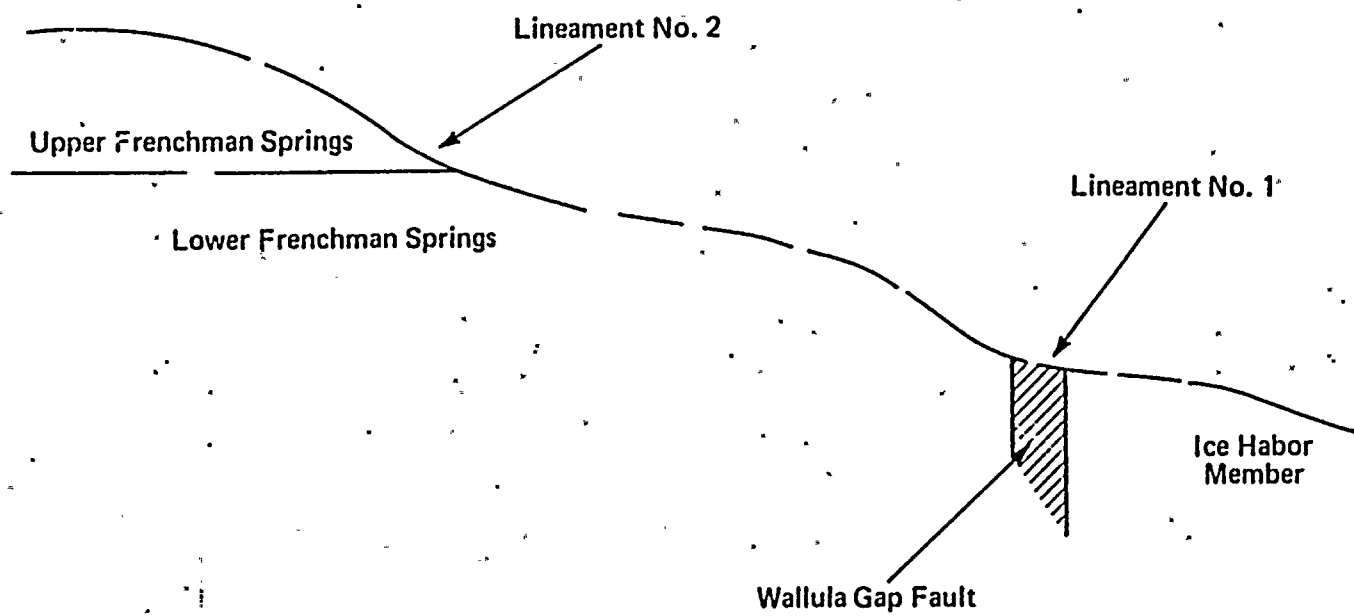






<p>WASHINGTON PUBLIC POWER SUPPLY SYSTEM</p> <p>Nuclear Project No. 2</p>	<p>LINEAMENTS NEAR THE MOUTH OF WARM SPRINGS CANYON</p>	<p>Figure 360.16-2</p>
---	---	----------------------------





<p>WASHINGTON PUBLIC POWER SUPPLY SYSTEM</p> <p>Nuclear Project No. 2</p>	<p>DIAGRAMATIC CROSS-SECTION THROUGH THE VICINITY OF THE WARM SPRINGS TRENCHES</p>	<p>Figure 360.16-3</p>
---	--	----------------------------



Q. 360.018

- . Describe the uniqueness of Toppenish Ridge that lead you to conclude that an earthquake (or earthquakes) like that which produced the young scarps on Toppenish Ridge is unlikely to occur on other folds closer to the site.

Response:

#### 1.0 Conclusions of Toppenish Ridge Investigations

The various investigations, to date, concerning the origin of topographic scarps on Toppenish Ridge have had differing approaches and differing levels of effort and detail. All of the studies have concentrated on reconnaissance level geomorphologic investigations and geologic mapping and none have utilized subsurface investigative techniques.

#### 1.1 Background of Previous Studies

The initial field work on the topographic scarps and geology of Toppenish Ridge was conducted in 1978 and 1979 by Newell Campbell and Robert Bentley and reported in Rigby and Othberg (1979), Bentley and others (1980), and Campbell and Bentley (1981). Campbell and Bentley (1981) report a zone of scarps 0.5 km to 2.2 km wide that extends 32 km along the north slope of the Status Peak anticline segment of Toppenish Ridge. The scarps occur in three sets: the crestal, hinge and fan sets. The crestal and hinge sets cross topography suggesting steep dips while the fan set is sinuous suggesting a gentle southerly dip. The scarps displace surfaces that are underlain by Miocene through Holocene age materials.

Bentley and others (1980), and Campbell and Bentley (1981) conclude that the topographic scarps present on Toppenish Ridge are likely to be tectonic features that formed at the same time as tectonic folding and thrusting, and that they record some of the latest north-south compressional deformation in the region. The scarps are probably related to uplift folding and thrusting of the Status Peak anticline segment of Toppenish Ridge as it moved northward along northwest-striking fracture systems (Campbell and Bentley, 1981). Campbell and Bentley (1981) further conclude that extension of the hinge area of the fold formed the hinge and crestal scarps while compression occurred at the base of the slope forming the fan set or thrust-line scarps. Although the scarps are probably tectonic in origin, this has not been conclusively proven and alternative non-tectonic origin include gravitational ridge spreading, landsliding, and ground-water withdrawal (Campbell and Bentley, 1981).

Based on a remote sensing analysis using small scale aerial photographs, Glass (1979) concluded that the most likely candidates for active faults associated with the Toppenish Ridge are the northwest-trending lineaments near the western portion of the ridge. He also concluded that the faults associated with the east-west anticline are probably not active; however, if they are active, the northwest-trending lineaments are also probably active. Based on the length and character of the zone of scarps observed during aerial reconnaissance, Glass (1981) concluded that the scarps are probably tectonic in origin but that a non-tectonic origin cannot be ruled out. In addition, he stated that the scarps on Toppenish Ridge are the youngest of any he has observed on the Columbia Plateau.

Based on aerial reconnaissance and preliminary analysis of the observed geomorphic character of the scarps, Kiel and Davis (1980) and Davis (1981) concluded that gravitationally induced slope failure is a viable alternative to a tectonic origin for the scarps on toppenish Ridge.

The results and conclusions from previous studies of Toppenish Ridge generally suggest a tectonic origin for the scarps that occur along a 30 km segment of the ridge. In general, the scarps are considered to be the result of primary movement of a thrust fault along the north base of Toppenish Ridge and secondary faulting within the upper slopes due to tectonic extension or gravitational adjustments within the overthrust block. In addition, the previous work has noted that the scarps appear to be confined to the segment of Toppenish Ridge that is separated from adjacent segments by, or related to, northwest-trending fractures and lineaments (Bentley and others, 1980; Campbell and Bentley, 1981; Glass, 1979). Although the general conclusion is that the scarps may be tectonic, there is still uncertainty in this conclusion, voiced by the previous workers, such that a non-tectonic origin cannot be precluded.

## 1.2 Results of Investigations by Applicant

The purpose of the applicant's studies (Woodward-Clyde Consultants, 1981) was to assess whether the scarps are non-tectonic or tectonic in origin and to assess the capability of scarps that were identified as being tectonic. The scope of work included a review of available data and literature, photogeologic interpretation of available aerial photographs, and aerial reconnaissance. Ground access to the Yakima Indian Reservation was restricted. Because of the lack of ground access, direct measurement of scarp heights, geometry, and slope morphology was not possible. Likewise, direct information related to bedrock structure and its relationship to the scarps is based on previous work by others.

The results of the applicant's investigations (Woodward-Clyde Consultants, 1981) concurred in general with results of previous investigations (Rigby and Othberg, 1979; Bentley and others, 1980). Woodward-Clyde Consultants (1981) reports that the zone of scarps on the north slope of Toppenish Ridge ranges from 1 to 2 km wide and extends a length of 24 km along the Satus Peak segment of the ridge. Three sets of scarps are identified: the crestal, midslope, and basal set. The basal set is the longest (24 km) and most continuous and is sinuous, following topography which suggests a gentle southerly dip. The crestal and midslope sets are less continuous and cut across topography suggesting steep dips. Two possible mechanisms for the primary origin of the scarps were identified (Woodward-Clyde Consultants, 1981):

- o gravitational failure (non-tectonic)
- o thrust faulting (tectonic)

It was concluded that the scarps observed on Toppenish Ridge are most likely tectonic in origin and because of the Holocene age of the scarps, they are considered capable. They were formed due to displacement on a low angle, south-dipping thrust fault. The thrust displacement occurred along the base of the north slope of Toppenish Ridge for a distance of 24 km. The midslope and crestal set scarps are secondary features formed either by gravitational adjustments in the overthrust block or by tectonic extension in the upper block (Woodward-Clyde Consultants, 1981). The 24 km-long zone of scarps occurs along the 30 km-long segment of Toppenish Ridge that coincides with the Satus Peak anticline, which was first described by Bentley and others (1980). Segments of Toppenish Ridge, which has a total length of 95 km, can be defined on the basis of stratigraphy, structure and geomorphology (refer to Question 360.019). Although the tectonic origin seems most likely based on the available data, a non-tectonic origin cannot be precluded because of the lack of detailed geologic and geometric data for the scarps.

## 2.0 Uniqueness of Toppenish Ridge

In a general sense, the folds of the Yakima fold belt have many stratigraphic and structural similarities and it is these similarities that have previously allowed the definition of the fold belt. However, each fold has unique geologic, structural and geomorphic characteristics that distinguish it from other folds. These variations in structural styles and fold development between the different folds reflect a spectrum of fault/fold relationships.



In general, Toppenish Ridge is different from the other east-west folds of the Yakima fold belt in the following ways:

- o The young topographic scarps observed on Toppenish Ridge have not been observed on other folds of the Yakima fold belt (Woodward-Clyde Consultants, 1981; Campbell and Bentley, 1981).
- o Association of the folds to regional northwest-trending strike slip faults (Bentley and others, 1980; Bentley and Anderson, 1979) has only been documented for the southwestern Yakima fold belt in the area of Toppenish Ridge.
- o Thrust faults having opposing dips have been mapped along both flanks of much of Toppenish Ridge and this is not common in the rest of the fold belt.
- o The location of Toppenish Ridge, west of longitude 120°, (in the western and southwestern portion of the Yakima fold belt) has undergone more north-south crustal shortening than to the east (Bentley, 1981).

Because of the variations in the style of deformation associated with different plateau folds, the seismic potential of each fold should be evaluated on the basis of its own structure and deformation. The characteristics of the structures closest to the site, the Rattlesnake, Wallula alignment and Umtanum Ridge, Gable Mountain structural trend, are summarized in response to Question 360.14 and 360.20 and deterministic assessments of the potential ground motions from these structures are made. The characteristics and seismic potential of these and all other plateau structures that extend to within a 50 km radius of the site are summarized in Amendment 18, Appendix 2.5K. The results of these analyses indicate that an event similar to the one that is assumed to have produced the scarps along Toppenish Ridge is unlikely on the other folds closer to the site.

#### References:

- Bentley, R.D., and Anderson, J.L. 1979, Right-lateral strike-slip faults in the western Columbia Plateau, Washington: Abstracts, EOS, v. 60, n. 46, p. 961.
- Bentley, R.D., Anderson, J.L., Campbell, N.P., and Swanson, D.A., 1980, Stratigraphy and structure of the Yakima Indian Reservation with emphasis on the Columbia River Basalt Group: U.S. Geological Survey Open-File Report 80-200, 79p.

- Bentley, R.D., 1981, Magnitude of Neogene Horizontal shortening in the western Columbia Plateau Washington - Oregon: Abstracts, EOS, v. 62, n. 6, p. 60.
- Campbell, N.P. and Bentley, R.D., 1981, Late Quaternary deformation of the Toppenish Ridge uplift in south-central Washington: Geology, v. 9, p. 519-524.
- Davis, G.A., 1981, Late Cenozoic tectonics of the Pacific Northwest with special reference to the Columbia Plateau: Appendix 2.5N to Final Safety Analysis Report WNP-2 and 1/4.
- Glass, C.E., 1979, Interpretation of U-2 and Forest Service photography, Letter to David Tillson, Principal Geologist, Washington Public Power Supply System regarding air photo interpretation of Toppenish Ridge.
- Glass, C.E., 1981, WPPSS Hanford Projects Remote Sensing Task C-9, Trip Report 2-21-81: Letter to John Doherty, Project Manager, Weston Geophysical Corporation regarding aerial reconnaissance of Toppenish Ridge.
- Kiel, W. and Davis, G.A., 1980, Unpublished field trip notes of aerial reconnaissance of Toppenish Ridge conducted 7/2 - 7/3/80.
- Rigby, J.G., and Othberg, K., 1979, Reconnaissance surficial geologic mapping of the Late Cenozoic sediments of the Columbia Basin, Washington: State of Washington, Division of Geology and Earth Resources, Open-File Report 79-3.
- Woodward-Clyde Consultants, 1981, Task D5 Toppenish Ridge Study: report prepared for Washington Public Power Supply System, 33 p.

Q. 360.020

Provide a summary of all prominent structures (other than those incorporated into Question 360.014 as part of the (CLEW) in the site region, discussing in detail their character and capability with supporting evidence for your judgement. If you determine any to be segmented, provide a map on topographic base delineating the segments and discuss in detail the character and capability of the individual segments with supporting basis.

Response:

The faults that may be potential seismic sources of significance to the site are those associated with the Rattlesnake-Wallula alignment (discussed in Question 360.014) and with the Umtanum Ridge-Gable Mountain structural trend. These structures are the closest to the site and, therefore, are the most significant to a deterministic assessment of ground motions at the site. In response to this question, the data regarding the tectonic models and segmentation of the Umtanum Ridge-Gable Mountain structural trend will be summarized, followed by a discussion of the capability, fault parameters, maximum magnitudes, and site ground motions for the potential seismic sources associated with the structural trend.

#### Tectonic Models and Segmentation

The data and interpretations regarding the Umtanum Ridge-Gable Mountain structural trend are summarized in 2.5.1.2.4.2 and 2.5.1.2.4.3 and are presented in detail in Golder Associates (1981a and 1981b). The principle conclusions of these studies regarding tectonic models and segmentation are summarized below:

- o The Umtanum Ridge-Gable Mountain structural trend is a segmented anticlinal high.
- o The structural trend is comprised of five segments (Figure 360.020-1) that are separated from each other on the basis of changes in the style of deformation and fold orientation. Individual segments show marked differences in fold vergence, fold amplitudes and widths, and development of first, second, and third-order folds.
- o The Umtanum fault and other east-west trending reverse faults are inferred to be products of fold deformation in a north-south compressional stress regime. Geologic

data support the hypothesis that the Umtanum fault was generated from the core of a concentric fold and that faulting is a direct result of folding on this structure. On this basis, the faults associated with Umtanum Ridge are discontinuous and confined to the length and width of individual fold segments.

- o Three prominent second-order folds are superimposed on the first-order fold that forms the Gable Butte-Gable Mountain segment of the Umtanum Ridge-Gable Mountain structural trend (Figure 360.020-2).
- o Faults associated with the Gable Butte-Gable Mountain segment are inferred to be the product of folding of the second-order folds. For this reason, fault lengths and widths are constrained by the dimensions of individual folds.
- o The southeast anticline segment of the Umtanum Ridge-Gable Mountain structural trend is interpreted to be a first-order fold of low amplitude that is separate from the Gable Butte-Gable Mountain segment.

#### Capability

The mapped faults along the Umtanum Ridge-Gable Mountain structural trend that will be considered in the assessment of capability are the Umtanum fault, the central fault on Gable Mountain, the north-dipping reverse fault on the west Gable Mountain anticline, and the southeast anticline fault.

The Umtanum fault has been investigated by Golder Associates (1981a) and no evidence of Quaternary faulting was observed. A fan conglomerate that is inferred to be at least 200,000 years old is not displaced where it was found to overlie bedrock faults (Golder Associates, 1981a). In addition, the absence of any marked geomorphic expression along most of the mapped length of the Umtanum fault in the study area suggest an absence of displacement during the late Quaternary on this structure (Golder Associates, 1981a). Based on these evaluations, the Umtanum fault is interpreted to be not capable.

The central fault on Gable Mountain displaces glaciofluvial deposits correlative with late-pleistocene Missoula flood deposits that are between 13,000 and 19,000 years old. The evidence indicates that the faulting may be coincident with the late Pleistocene floods, which suggests that the faulting may have been flood induced. Although some evidence supports



nontectonic hypotheses for the origin of the displacements in the glaciofluvial deposits, data gathered to date are insufficient to demonstrate a nontectonic mechanism for the origin of the observed displacement (Golder Associates, 1981b). Based on these data, the central fault is interpreted to be capable, within the criteria of 10CFR100.

The existence of the north-dipping reverse fault on the west Gable Mountain anticline is inferred from borehole data and no information is available for directly assessing its capability. The south fault is interpreted to be antithetic to the north-dipping reverse fault (Golder Associates, 1981b), although the data are insufficient to confirm this association. Assuming an antithetic relationship, data on capability of the south fault may allow inferences regarding the capability of the north-dipping reverse fault. The south fault does not displace overlying glaciofluvial deposits; however, slickensides in clastic dikes that are apparently derived from these deposits suggest minor dip-slip displacement has occurred on the south fault since dike emplacement (Golder Associates, 1981b). This displacement may have been flood induced but tectonic movement cannot be disproved. Because the south fault is inferred to be a minor, antithetic fault in the hanging wall of the north-dipping reverse fault (Golder Associates, 1981b), it is not considered for magnitude assessment.

Because of the uncertainties in the capability of the south fault and its relation to the north-dipping reverse fault, the capability of the north-dipping reverse fault is uncertain. However, because of the possible structural relationship between the north-dipping reverse fault and a presumed capable fault (the south fault), the north-dipping reverse fault may be interpreted to be capable, within the criteria of 10CFR100, and resultant magnitudes and grand motions are therefore discussed below.

A fault has been inferred along the southwestern flank of the southeast anticline from borehole and geophysics data (Figure 360.020-2). Several aspects of the relationship between the Gable Butte-Gable Mountain segment and the southeast anticline indicate that the southeast anticline is a separate first-order fold segment. The bases for this conclusion are presented in Golder Associates (1981b) and are summarized here: 1. a saddle defined from gravity data in the buried basalt surface at the east end of Gable Mountain separate the segments, 2) the southeast anticline extends about 1.6 km to the northwest beyond the eastern end of the Gable Butte-Gable Mountain segment, 3) the Gable Butte-Gable Mountain segment is bounded on the east by the May Junction monocline, and 4) there is a marked change in trend of the first-order fold segments from nearly east-west (Gable Butte-Gable Mountain segment) to approximately N45°W (southeast anticline segment).



As presented in the FSAR Amendment 18 (Section 2.5.2.4.2.2), the preferred estimate of the maximum earthquake magnitude for the central fault on Gable Mountain is M 5. Based on the parameters presented above for the north-dipping reverse fault, the area-magnitude relationship (presented in response to Q. 360.014) yields magnitudes of 3.9 to 5.1 ( $\pm 0.3$ ). The length - magnitude relationship is not considered applicable for rupture lengths as short as 3 km and, therefore, is not used in estimating maximum magnitude. The preferred estimate of maximum magnitude for the north-dipping reverse fault is M 5. As presented in the FSAR Amendment 18 (Section 2.5.2.4.2.2), the maximum magnitude for the central fault is M 5.

Two important points should be considered in evaluating these maximum magnitude estimates: 1) the seismogenic character of these faults and, 2) the applicability of the fault parameter - magnitude relationships. Although the central fault is considered to be capable and the north-dipping reverse fault is treated here as being capable according to 10CFR100 criteria, their tectonic role as secondary faults related to relatively minor second-order folds, their limited physical dimensions, their lack of correlation with historical seismicity, and possible non-tectonic origins for the displacement in the flood deposits raise questions regarding their potential to generate earthquakes. The estimated maximum dimensions of these faults is well below the empirical data base typically used for making magnitude estimates (see response to Q. 360.014). For example, the smallest magnitude and associated rupture length in the reverse fault data set of Slemmons (1977) is  $M_L$  7.1 associated with a 20 km rupture length. Extrapolation of this relationship back to rupture lengths as short as 1/2 km to 3 km is inappropriate, and Slemmons (1977) attempts to discourage such extrapolations by defining a "boundary of applicability" to his relationships. The fault area - magnitude relationship is considered valid for  $M > 5.7$  (Wyss, 1979), but the fault dimensions associated with M 5.7 are still greater than those proposed for the central fault and north-dipping reverse fault.

#### Ground Motions

The ground motions resulting from a M5 earthquake on the central fault at a distance of 18 km is discussed in FSAR Amendment 18 (Section 2.5.2.6.1). The estimated peak acceleration at the plant site for this earthquake is less than 0.1 g. The north-dipping reverse fault is also at a distance of 18 km from the site and is also assessed a maximum magnitude of 5; therefore, the site ground motions are the same.



## WNP-2

Because of their close proximity to the WNP-2 and WNP-1/4 site relative to other plateau structures, the most likely source for an SSE is either the Rattlesnake-Wallula alignment discussed in response to Question 360.014 or the Umtanum Ridge-Cable Mountain structural trend discussed above. This is confirmed by the Seismic Exposure analysis which includes an analysis of all plateau structures within a 50 km radius of the site (see Amendment 18, Appendix 2.5 K, WNP-2 FSAR).

There is uncertainty regarding the nature of plateau deformation and the seismic potential of the structures in the site region. Because of these uncertainties conservative assumptions have been made in the deterministic assessments of the capability of the potential sources of the SSE. Although tectonic models can be postulated that might suggest these faults have greater seismic potential, these models are only permissive and not supported by the weight of available geologic and seismic evidence in the Columbia Plateau. Alternative tectonic models and their significance to the SSE are evaluated in the WNP-2 FSAR, Amendment 18, Appendix 2.5K.

### References:

- Fulton, R.G., and Smith, G.W., 1978, Late Pleistocene stratigraphy of south central British Columbia: Canadian Journal of Earth Science, v. 15, p. 971-980.
- Golder Associates, 1981a, Geologic structure of Umtanum Ridge: Priest Rapids Dam to Sourdough Canyon: Appendix 2N, Skagit/Hanford Nuclear Project Preliminary Safety Analysis Report, for Northwest Energy Services Company, 44 p.
- Golder Associates, 1981b, Gable Mountain: Structural Investigations and Analyses: Appendix 2O: Skagit/Hanford Nuclear Project Preliminary Safety Analysis Report, for Northwest Energy Services Company, 58 p.
- Waite, R.B., Jr., 1980, About forty last-glacial Lake Missoula jokulhaups through Southern Washington: Journal of Geology, v. 88, p. 653-679.
- Webster, G.D., and Crosby, J.W., III, 1981, Stratigraphic investigation of the Skagit/Hanford Nuclear Project: Preliminary Safety Analysis Report, Appendix 2R, Northwest Energy Services Company, Kirkland, WA.

The results of investigations by Webster and Crosby (1981) that relate to the assessment of the capability of the southeast anticline fault are summarized below. The fault is inferred from the borehole data by a thickening of the Elephant Mountain basalt (10.5 m.y. old) and by several thin (maximum thickness approximately 1 m) shear zones within this anomalously thick section. Cumulative vertical displacement of this unit is no more than about 30 m. The overlying Ringold section is anomalously thin along the inferred trend of the fault but it is not clear whether Ringold sediments are deformed by the fault. The Ringold section in the southeast anticline area is interpreted to be between 3.3 and 10 million years old. No deformation is recognized in the pre-Missoula flood gravels nor the Missoula flood gravels across either the southeast anticline or the southeast anticline fault. The Missoula flood deposits are estimated to be 13,000 to 19,000 years old (Fulton and Smith, 1978; Waitt, 1980). The age of the pre-Missoula deposits is not known, but they may be as old as the youngest underlying Ringold formation (approximately 3 million years old). Possibly correlative flood deposits have yielded dates on the order of several hundred thousand years (Webster and Crosby, 1981). Neither the southeast anticline nor the fault along its flank have any geomorphic expression. Although the data regarding capability are somewhat limited, the available evidence supports the interpretation that the southeast anticline fault is not capable.

#### Fault Parameters and Maximum Magnitudes

The magnitude-related fault parameters for the central fault on Gable Mountain are presented in the FSAR Amendment 18 (Section 2.5.2.4.2.2). Fault parameters for the north-dipping reverse fault on the west Gable Mountain anticline are presented in this section. The north-dipping reverse fault is known from borehole data over a length of about 1 km. The fault is interpreted to be the product of folding of the west Gable Mountain anticline (Golder Associates, 1981b); therefore, its maximum inferred length is the total length of the anticline, 6 km. Assuming a rupture length of one-half the total length, the rupture length may be 1/2 km to 3 km. Downdip fault width may be estimated from known fold geometry. The maximum fold amplitude of the Gable Mountain anticline is about 300 m. The width (wavelength) of the west Gable Mountain anticline is less than 1 km. A shallow-dipping fault associated with this fold would probably have a width of less than 1 km, and certainly less than 3 km. In summary, the magnitude-related fault parameters for the north-dipping reverse fault are:

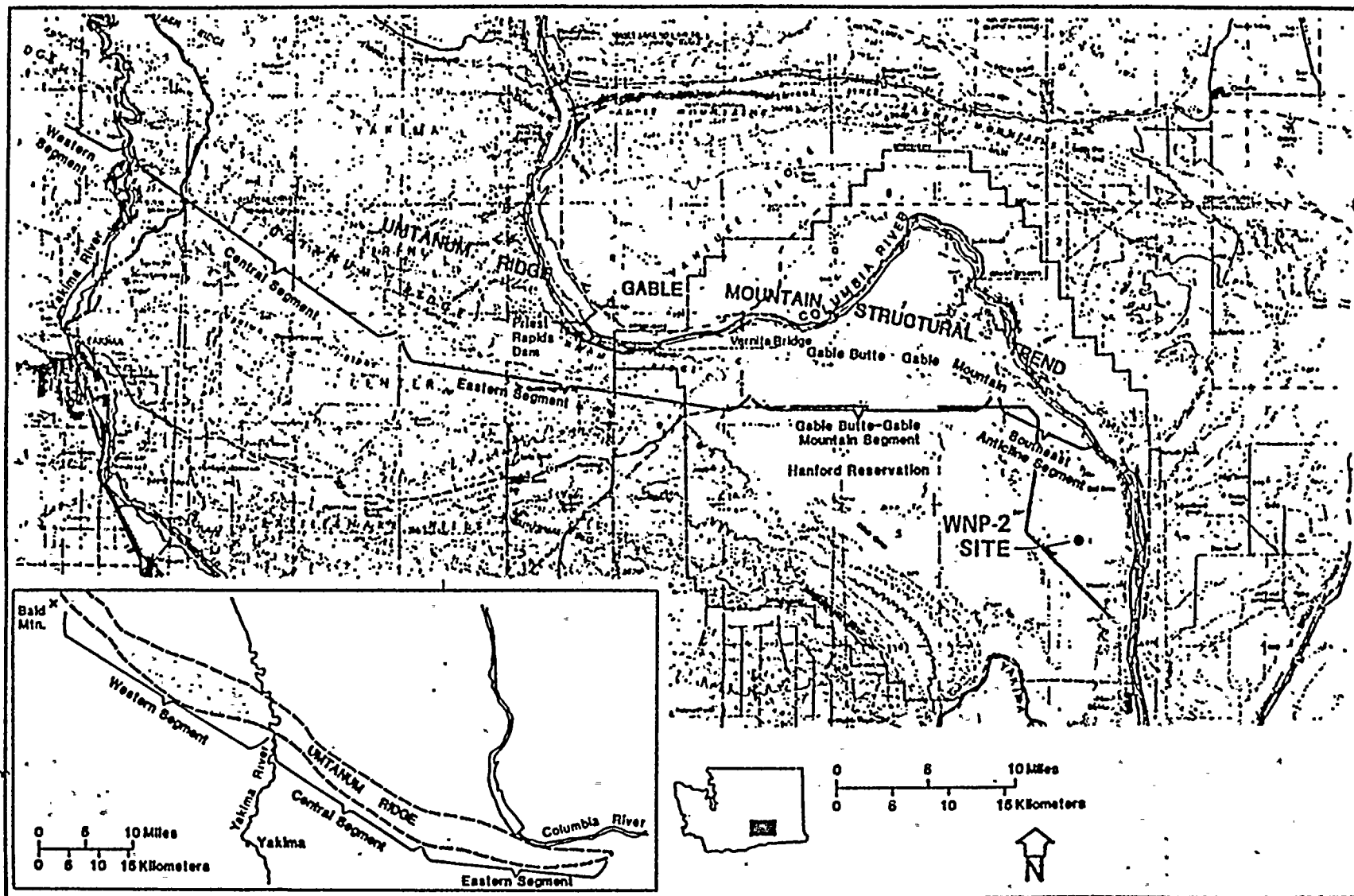
Total Length	1 - 6 km
Rupture Length	1/2 - 3 km
Fault Width	1 - 3 km



WASHINGTON PUBLIC  
POWER SUPPLY SYSTEM  
Nuclear Project No. 2

MAP OF UMTANUM RIDGE-GABLE  
MOUNTAIN STRUCTURAL TREND  
SHOWING SEGMENTS  
(From Golder Associates, 1981a)

Figure  
360.20-1

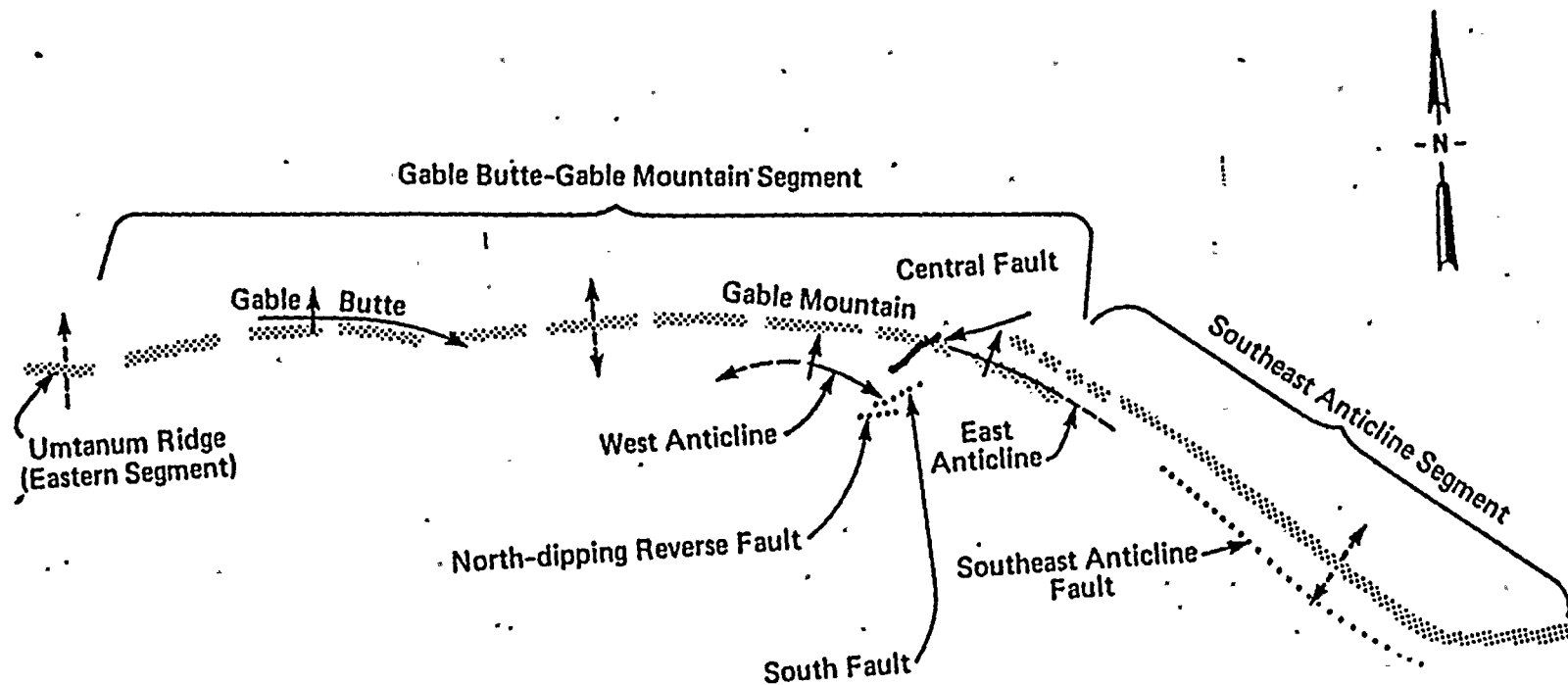




WASHINGTON PUBLIC  
POWER SUPPLY SYSTEM  
Nuclear Project No. 2

MAP OF GABLE BUTTE-GABLE MOUNTAIN  
AND SOUTHEAST ANTICLINE SEGMENTS  
OF THE UMTANUM RIDGE-  
GABLE MOUNTAIN STRUCTURAL TREND

Figure  
360.20-2



0 1 2 mi  
0 1 2 3 km



WNP-2

Q. 360.021

Provide the letter report and lineament maps from C. Glass to WPPSS of lines of aerial reconnaissance of Toppenish Ridge. (Contact Ina Alterman, GSB, 301-492-7856)

Response:

The letter report from Dr. Charles E. Glass to Mr. D. D. Tillson (Washington Public Power Supply System) dated October 3, 1979 was mailed to Dr. Ina Alterman November 24, 1981. Upon receipt of that material, the air photos used in the original analysis plus the transparent overlay prepared by Dr. Glass were also requested. This material was transmitted to Dr. Alterman on December 22, 1981.





Q. 361.018

Provide a discussion on how, and at what stage, uncertainty was accounted for in the seismic exposure analysis (including graphical examples).

Response:

Two kinds of uncertainty are considered in the evaluation of seismic exposure at the Hanford site, inherent uncertainty and statistical uncertainty. Inherent uncertainty refers to the situation where a future outcome of a process cannot be predicted with certainty even if a large amount of historical data is available. For the present study, the uncertainty in predicting the actual time and location of future earthquakes and the resulting level of ground motion constitutes inherent uncertainty. Statistical uncertainty consists of uncertainty in the process parameters which may be resolved or reduced with additional data. In the analysis described in Appendix 2.5K, the parameters which define the potential earthquake sources are treated as statistically uncertain. These parameters are source segmentation, capability, tectonic model, geometry, maximum magnitude, and recurrence rate.

The basic exposure calculation includes the inherent uncertainty in the time and place of earthquake occurrence and the generation of strong ground motion to estimate the probability of exceeding a specified level of ground motion at the site. The occurrence of earthquakes on a source is assumed to be a Poisson process. The probability of the occurrence of at least once event in a specified time period,  $t$ , is given by the equation

$$p(\geq \text{zero events}) = 1 - e^{-\lambda t} \quad (1)$$

where  $\lambda$  is the mean rate of occurrence of earthquake on the source.

Assuming that the probability of any one event resulting in ground motions at the site in excess of a specified level is independent of the occurrence of other events, the occurrence of ground motions at the site is also a Poisson process. The probability of ground motion parameter  $Z$  exceeding a specified level of  $z$  is given by

$$p(Z > z) = 1 - e^{-v(z)} \quad (2)$$

in which  $v(z)$  is the mean rate of occurrence of events in time  $t$  in which ground motion level  $z$  is exceeded. For simplicity,  $v(z)$  is termed the mean rate of exceedence. In the exposure is given by the expression

$$v(z) = \sum_i t \cdot \lambda(m_i) \cdot \sum_j p(R = r_j | m_i) \cdot p(Z > z | m_i, r_j) \quad (3)$$

The mean rate of occurrence,  $\lambda(m_i)$ , of magnitude  $m_i$  earthquakes, is given by the expression

$$\lambda(m_i) = A_n \cdot \left[ \frac{e^{-b \cdot 1n10 \cdot (m_i - \Delta m - m^0)} - e^{-b \cdot 1n10 \cdot (m_i + \Delta m - m^0)}}{1 - e^{-b \cdot 1n10 \cdot (m^u - m^0)}} \right] \quad (4)$$

Where  $m^u$  is the maximum magnitude possible on the source,  $m^0$  is the minimum magnitude considered in the analysis,  $\Delta m$  is a suitable discretization step,  $b$  is the slope of the magnitude frequency relationship and  $A_n$  is the mean rate of occurrence of earthquakes of magnitude greater than  $m^0$  on the source.

The uncertainty in the location of the earthquake on the source is characterized by assuming a uniform distribution for the location of the rupture surface. This is shown schematically in Figure 361.18-1a.

The probability of exceedence given a particular magnitude and distance is calculated from the distribution about the median estimate of attenuation of ground motion, as shown in Figure 361.18-1b. By summing over all possible magnitudes and distances, a mean rate of exceedence is calculated which expresses the inherent uncertainties in a Poisson process.

The exposure model used in the analysis for the Hanford site was expanded to include statistical uncertainties in the input parameters to equations (3) and (4). This was accomplished by treating the rate of exceedence,  $v(z)$  as a random variable and considering the uncertainty in  $v(z)$  as resulting from uncertainty in the source definition parameters  $A_n$ ,  $m^u$ , and source geometry.

Uncertainty in source geometry and maximum magnitude was characterized by constructing a logic tree representing the possible states of the various input parameters. The logic tree constructed for Saddle Mountains is shown in Figure 361.18-2. The end branches of the logic tree define a discrete joint distribution for fault geometry and maximum magnitude.

The procedure used to calculate the distribution for the exceedence rate  $v(z)$  is illustrated schematically in Figure 3. For each state of maximum magnitude and fault geometry defined by an end branch of the logic tree in Figure 361.18-2 an exceedence rate was calculated using equations (3) and (4) and the expected value of  $A_n$  for the source. The result is a discrete distribution for  $v(z)$  conditional on the expected value of  $A_n$ . This distribution is shown in Figure 361.18-2a.



The parameter  $A_n$  is considered to be lognormally distributed. Values of  $A_n$  different from its mean value would result in different values of  $v(z)$ . Thus, as shown in Figure 361.18-3b each mass point in Figure 361.18-3a can be expanded into a distribution. As the distribution due to  $A_n$  is assumed to be independent of the joint distribution on  $m^{un}$  and fault geometry, the individual distributions shown in Figure 361.18-3b can be summed to produce the final unconditional distribution shown in Figure 361.18-3c.

Shown in Figure 361.18-3 is the mean or expected value of  $v(z)$  both for the conditional distribution in (Figure 361.18-3a) and the unconditional distribution in (Figure 361.18-3c). Because of the linearity of equations (3) and (4) in  $A_n$ , the means of the two distributions are identical. The effect of including uncertainty in the recurrence rate  $A_n$  is to widen dispersion about the mean as shown by the mean plus one standard deviation values in Figure 361.18-3.

The final step in the analysis is the calculation of the probability of exceedence. In the case of low probability levels ( $<.01$ ) the probability of exceedence is essentially equal to the rate of exceedence.

$$p(Z > z) = 1 - e^{-v(z)} \approx v(z) \quad (5)$$

This result holds for any probability distribution. Thus for small values of  $v(z)$ ; the assumption of a Poisson distribution is not critical. The distribution derived in Figure 361.18-3 for the exceedence rate applies also to the probability of exceedence.

The methodology used in Appendix 2.5K is very similar to that proposed in NUREG/CR-1582, vol. 2. As described in Appendix A of NUREG/CR-1582, vol. 2, statistical uncertainty in the input parameters is treated by defining a state vector of the possible states of the input parameters. In the analysis conducted for the Hanford site, the possible states of the input parameters are defined by the end branches of the logic tree.

Thus, both methodologies define a distribution for the rate of exceedence similar in form to those shown in Figure 361.18-3; relying on subjective probability to calculate the probabilities assigned to individual states. The best estimate of the rate of exceedence is calculated in the same way for both methodologies, by summing over all possible states the exceedence rate calculated for each state multiplied by the probability of that state.

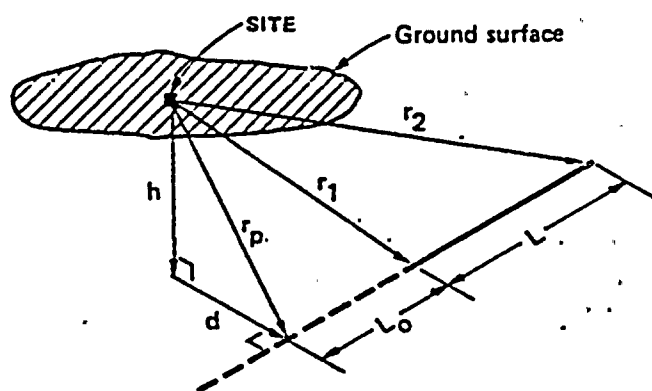
In addition to the best estimate or expected value of the rate of exceedence, other probability levels can be examined within the distribution. The 90% confidence level reported in Appendix 2.5K represents the level of exceedence rate below which 90% of the calculated probabilities of exceedence lie. This level is shown in Figure 361.18-3 for the unconditional distribution. Similar probability levels could also be reported for the distributions on exceedence rate developed in NUREG/CR-1582, vol. 2.

In summary, the distributions on exceedence rate derived in Appendix 2.5K represent statistical uncertainty in the input parameters for source definition. The inherent uncertainty in time and location of future earthquakes and attenuation of ground motions is used to calculate point estimates of exceedence rate for individual states of the input parameters.

#### REFERENCES:

TERA Corporation, 1980, Seismic Hazard Analysis; A Methodology for the Eastern United States: U.S. Nuclear Regulatory Commission, NUREG/CR-1582, v. 2, July 1980.





$$P(R < r) = 0$$

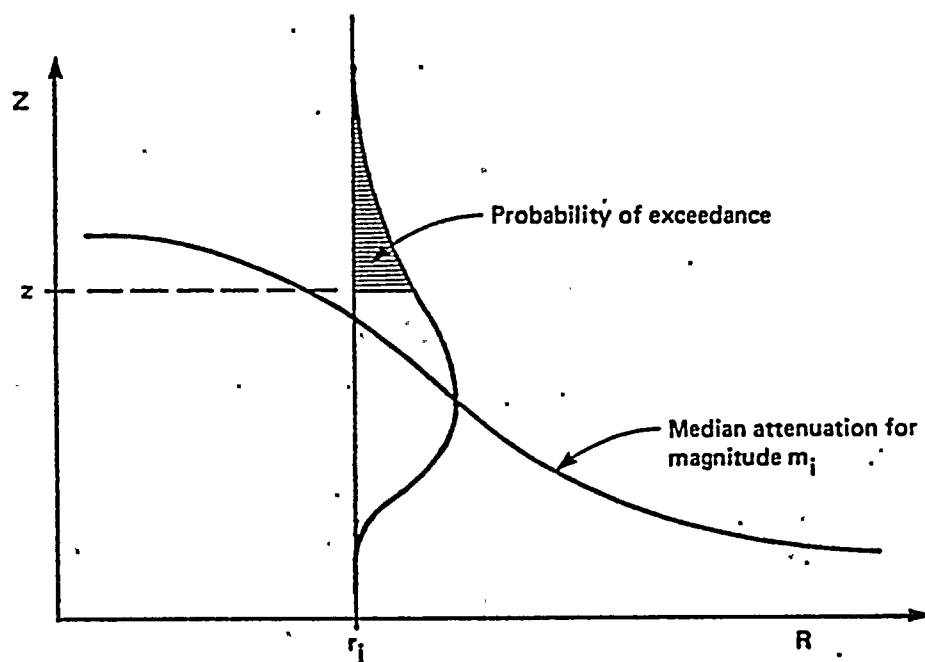
$$\text{for } r < r_1$$

$$= \frac{\sqrt{r^2 - r_p^2} - L_0}{L - L_{m_i}} \quad \text{for } r_1 < r < r_2$$

$$= 1$$

$$\text{for } r < r_2$$

a) Cumulative Probability Distribution for Closest Distance to Fault Rupture for Case of Fault Lying Completely on One Side of Site

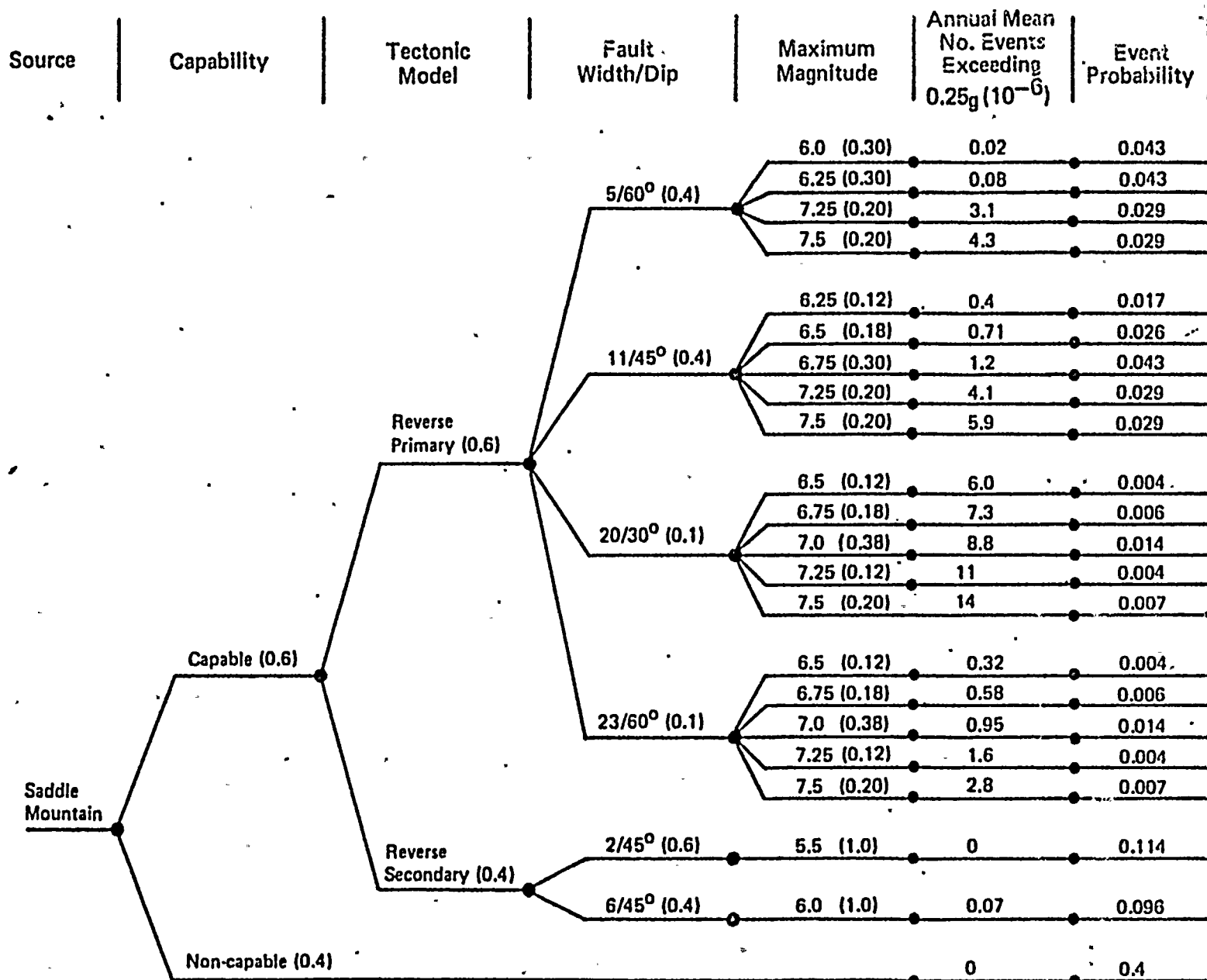


b) Conditional Probability of Exceedance

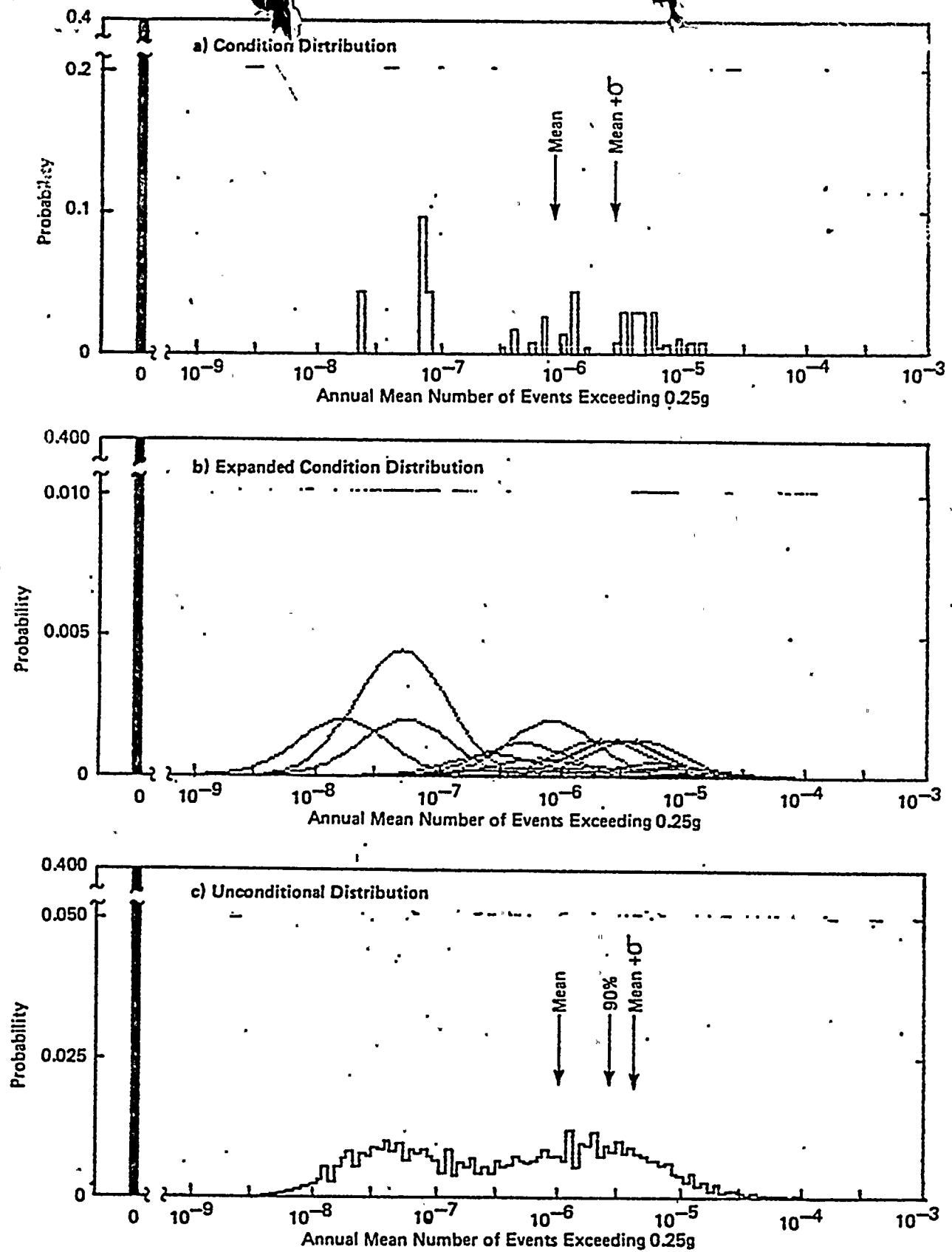
<p>WASHINGTON PUBLIC POWER SUPPLY SYSTEM Nuclear Project No. 2</p>	<p>SCHEMATIC OF TREATMENT OF INHERENT UNCERTAINTY IN EXPOSURE MODEL</p>	<p>Figure 361.18-1</p>
--	---	----------------------------











WASHINGTON PUBLIC  
POWER SUPPLY SYSTEM  
Nuclear Project No. 2

EXCEEDANCE RATE DISTRIBUTION FOR  
SADDLE MOUNTAINS

Figure  
361.18-3

